16th World Conference on Earthquake Engineering, 16WCEE 2017
Santiago Chile, January 9th to 13th 2017
Paper N° 1980
Registration Code: S-X1463185312

ASSESSMENT OF DYNAMIC SOIL PROPERTIES EFFECTS ON THE TRIGGERING ON SLOPE INSTABILITIES

M.E. Rahhal[(1)], A. Ghossoub[(2)]

[(1)] Professor, Saint Joseph University, Faculty of Engineering (ESIB), Lebanese Center for Studies and Research in Construction (CLERC), Beirut, Lebanon, muhsin.rahal@usj.edu.lb
[(2)] Researcher, Saint Joseph University, Faculty of Engineering (ESIB), Lebanese Center for Studies and Research in Construction (CLERC), Beirut, Lebanon, clerc.esib@usj.edu.lb

Abstract

Landslide effects have been numerous on infrastructures and on human lives, and their consequences during an earthquake might be a disaster. The pan Arab highway is a project comprising a network of roads binding the Middle East countries together. In the Lebanese mountains, in the Dahr el Baidar area and over the past twenty years, many slope instabilities and failures caused great damages in the highway projected area and other surrounding roads. This region is much known for its tectonic activity due to the fact that it is limited in the east by the major fault of Yammouneh, extension of the Dead Sea fault that crosses the Middle East, and by many minor faults in the west. Hundreds of boreholes have been executed and many geotechnical studies show that rain as well as presence of poor soil are two main causes of these landslides in the area.

The purpose of this research work is to evaluate how a slope will behave under seismic loading, and how the factor of safety and the slip circle will vary during an earthquake, with a special attention given to the role of dynamic soil properties in understanding slope instabilities. First, it has been proven that the amplification period and the amplification value itself at surface depend on the dynamic properties of the soil profile. Indeed, the amplification varies differently with a change in the maximum shear modulus, shear modulus reduction curve and damping curve. In addition, increasing the shear modulus and reducing the damping would lower the amplification values at surface.

Furthermore, this study showed that, while increasing the parameters of a single soil layer at surface, the slip circle will move to a different layer with weaker properties. Moreover, while increasing the parameters of soil layers in depth – in other words while increasing the stiffness contrast between surface and deep layers – the displacement of slip circle will not be observed, but the factor of safety will be reduced by 55% in some cases.

It is interesting to see how amplification of acceleration in time domain will depend on mechanical and dynamic proprieties of the soil, whereas amplification of RRS in frequency domain will only depend on the layer height above rock and the rock's acceleration response spectrum.

Keywords: slope stability, dynamic properties; shear modulus; earthquake acceleration.

1. Introduction

Landslide damages have been very noteworthy both on infrastructure and on human lives. Deaths due to landslides have increased lately, particularly in landslide-prone developing countries. Some progress has been made in building up techniques to minimize the probability of occurrence of landslides, although new, more efficient, quicker and cheaper methods could well emerge in the future [1]. The Lebanese mountainous topography and its different aquifers are among the principal reasons for a landslide risk [2, 3, 4]. In this study, landslides that occur on the pan Arab highway are considered, precisely in Dahr el Baidar area. In fact, this region is located between 1000 and 2000 m altitude above sea level, is subjected to a rate of rainfall ranging between 1100 and 1700 mm and has a mountainous Mediterranean climate.

The purpose of this research is to evaluate the importance of soil dynamics properties on a landslide and to understand how a slope will behave under seismic loading. A maximum peak horizontal acceleration a_{max} = 0.35g, will be considered as shown in the Lebanese contour map of maximum acceleration [5]. Next, an overview of the project and the available geotechnical data will be presented. Afterwards, a detailed analysis of the results as well as some conclusions will be given.

2. Overview of the project

First, in the screening investigation at the exploration phase [6], boreholes executed in Dahr el Baidar are analyzed in order to obtain an unambiguous idea concerning the nature of the soil layers. The boreholes showed that the soil profile could be divided in two main groups of layers; a first group of layers (mainly marl or clayey marl) at the surface that was soft with weak mechanical parameters and a deeper group of layers of stiff formation (mainly limestone and sandstone) with stronger mechanical parameters. The slip circle of all the landslides seems to be tangent to the interface of these two groups of layers with a high contrast of parameters.

Second, based on geotechnical data, several sections of the highway are made. Knowing that each section refers to a different area, this study will be based on a section that shows the biggest instability. Fig. 1 shows the topographic map of a chosen area in Dahr el Baidar, in addition to all sections.

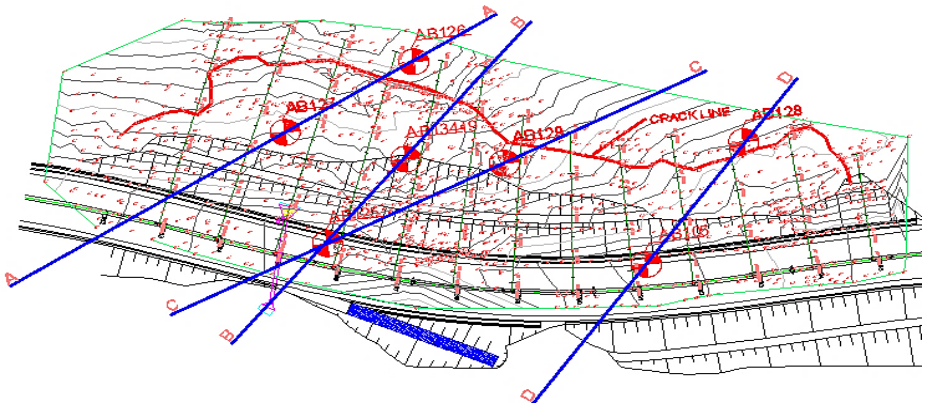

Fig. 1 – Topographic map showing sections and boreholes

The detailed analysis of section C – C shows that four major layers may be identified in the soil profile, as described in Table 1, and composed of: a layer of soft Marl with a very low plasticity index, a layer of Clayey Marl with low SPT N values, a layer of Marl and fractured Limestone with a higher plasticity index value and a good cohesion and finally a dense sand with high SPT N values becoming sandstone with depth. Values appearing in Table 1 were selected and calculated based on both in situ and laboratory soil investigation data.

Table 1 – Description of soil layers

Layer	Classification	c (kPa)	φ (°)	SPT	γ (kN/m³)	PI (%)
Marl	ML	22	23	9	1.8	10
Clayey Marl	CL	32	18	11	1.9	16
Marl and fractured Limestone	CL – ML	28	24	25	1.9	14
Sand, silt, Sandstone	SM	10	40	45	2.0	–

The section C – C is represented in Fig. 2 below. In order to understand the behavior of the soil during an earthquake, and to analyze the spectral response at the surface, this study will focus on three specific points at the surface as shown on Fig. 2. The first point (1) is not influenced by the clayey marl layer, the second point (2) is above all the layers, and the third point (3) isn't influenced by the marl layer on the surface. The location of each point is very important to determine which soil is influencing the most the seismic response of the slope.

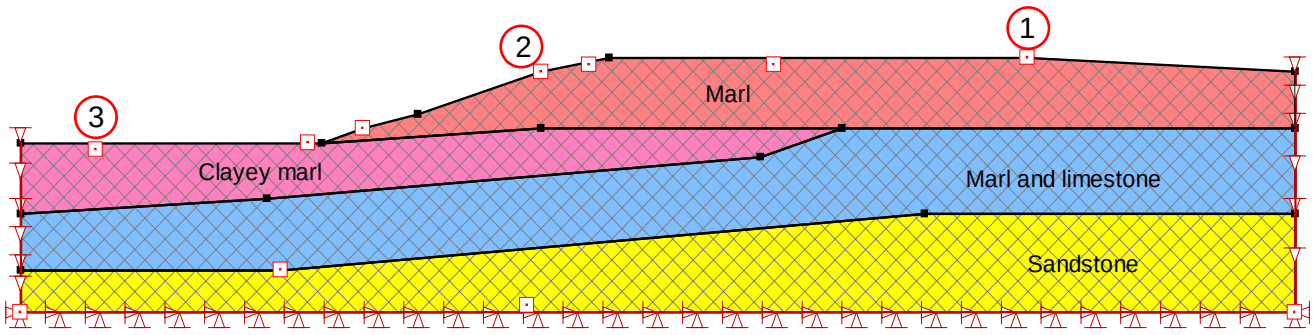

Fig. 2 – Section C – C with the location of the three points at the surface

3. Evaluating the effect of the dynamic soil parameters

In this section, we will emphasize on the dynamic parameters G_{max}, G/G_{max} and damping ratio of the soil, and determine their effects on the surface of the section C – C. In the calculations, the accelerogram produced by the El Centro earthquake will be considered; it happened in 1940 in California with a 6.6 magnitude, and lasted 10 seconds.

3.1 Effect of G_{max}

The low strain shear modulus G_{max} is a function that varies with the soil type of each layer. Before proceeding with our simulation, the value of G_{max} for each layer of the section C – C must be calculated.

In order to calculate G_{max}, two different equations depending on the soil type are used: Eq. (1) developed by [7] will be used for granular of soil layer, whereas Eq. (2) developed by [8], will be considered for cohesive soil.

$$G_{max} = 1000 K_{2,max} \times \sqrt{\sigma'_m} \quad \text{with } \sigma'_m = \sigma'_v \times \frac{1+2K_0}{3} \tag{1}$$

Making an assumption that the soil is isotropic, the values established by Seed and Idriss [7] for $K_{2,max}$ are used. As the layer of Sand, Silt and Sandstone, is considered to be a very dense sand, the magnitude of $K_{2,max}$ will be taken equal to 75.

$$G_{max} = 625 \left(\frac{1}{0.3+0.7e^2}\right) \times OCR^k \sqrt{P_a \sigma'_m} \quad \text{with } k = \frac{PI^{0.72}}{50} \tag{2}$$

Therefore, in order to calculate the values of G_{max}, the maximum depth of each layer should be determined, as well as the OCR value, the plasticity index and the $K_{2,max}$ value. All input data is shown in Table 2 below, as K_0 is taken equal to 1 for an isotropic soil. Calculated values of G_{max} are shown in Table 3.

Table 2 – Description of soil layers

Layer	Max depth (m)	$K_{2,max}$	OCR	PI (%)	σ'_m (kPa)
Marl	9.5	–	1	10	73
Clayey Marl	13.5	–	1	16	107
Marl and Limestone	21	–	1	14	172
Sandstone	34	75	–	–	297

3.1.1 Increasing the value of G_{max} for all the layers at once

To start with the sensitivity study, we have chosen to increase the values of G_{max} for all layers at once, in order to appreciate the effect of increasing rigidity on the slope stability response. Both initial and final G_{max} values are shown in Table 3.

Table 3 – Values of Gmax

	Marl	Clayey marl	Marl and Limestone	Sand, Silt and Sandstone
Initial values of $G_{max,i}$ (MPa)	53	65	82	283
Final values of $G_{max,f}$ (MPa)	159	195	246	849

From Eq. (3), increasing the values of G_{max} will lead to an increase of the values of V_s. With Eq. (4), an increase of V_s will decrease the fundamental period of the soil. Fig. 3 shows spectral acceleration response spectra.

$$G = \rho \times V_s^2 \tag{3}$$

$$T = \frac{4H}{V_S} \tag{4}$$

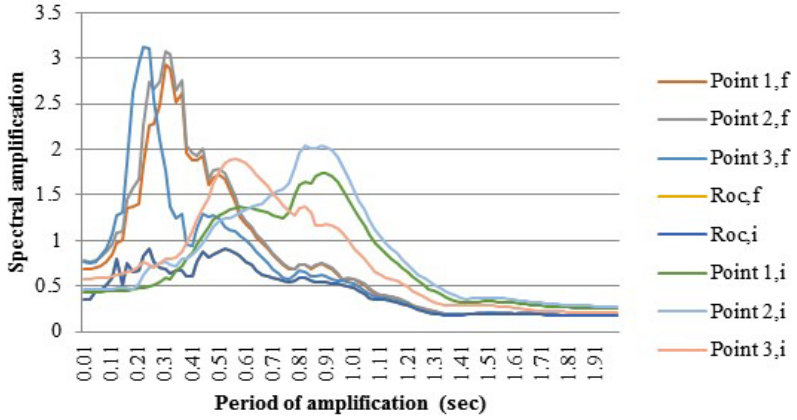

Fig. 3 – Spectral acceleration response for each point at the surface, with initial and final values of Gmax

The spectral acceleration response in Fig. 3 shows a decrease of the amplification period of the soil in the three points at the surface. Amplification period in the point 3 is always lower than the points 1 and 2. This is explained by the fact that an additional layer of soil is present under the points 1 and 2, which leads to a higher value of H in Eq. (4). Therefore, the value of the amplification period T for the points 1 and 2 will be higher than its value for the point 3, the other parameters being left constant. On the other hand, Fig. 3 shows a higher amplification for points 2 and 3 when compared to point 1, both for initial and final Gmax values.

3.1.1 Increasing the value of G_{max} for each layer separately

After increasing the values of G_{max} for all the layers together, we are now interested in the effect of increasing the value for each layer of soil independently, as shown in Table 4. Five scenarios may be observed (cases 0, 1, 2, 3, and 4). Therefore, the acceleration spectral response is drawn for each case and been combined in a single graphic, for each point at the surface.

The acceleration response spectra depend definitely on geotechnical conditions [9]. The increase of of G_{max} values in each layer separately has an interesting result. In the surface layers (case 1 and 2), the amplification depends on the nature of the layer. In fact, Fig. 4 shows amplification for point 1, as the Fig. 5 and Fig. 6 show a desamplification for the points 2 and 3.

Table 4 – Value of Gmax for each scenario (case)

Case number	Marl	Clayey marl	Marl and limestone	Sandstone
0	53 MPa	65 MPa	82 MPa	283 MPa
1	106 MPa	65 MPa	82 MPa	283 MPa
2	106 MPa	130 MPa	82 MPa	283 MPa
3	106 MPa	130 MPa	164 MPa	283 MPa
4	106 MPa	130 MPa	164 MPa	566 MPa

In conclusion, the increase of G_{max} at a surface layer of granular soil will increase amplification phenomena, as its increase in a cohesive soil will reduce it. In all cases, the amplification period stays the same. As the point 1 is not located above the clayey marl layer, the curves for cases 1 and 2 do not differ from each other.

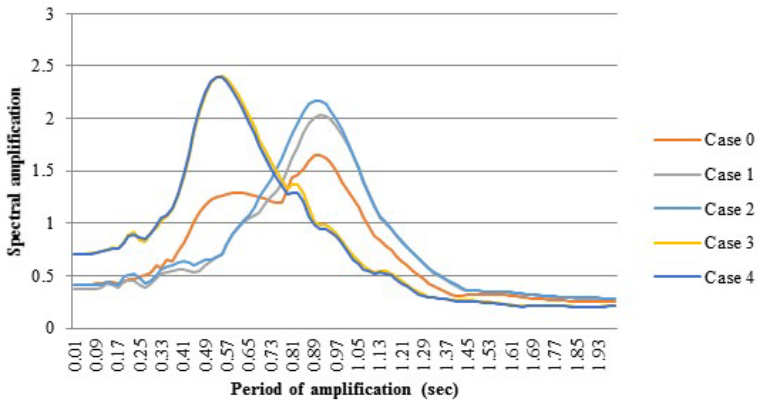

Fig. 4 – Spectral response for each case at point 1

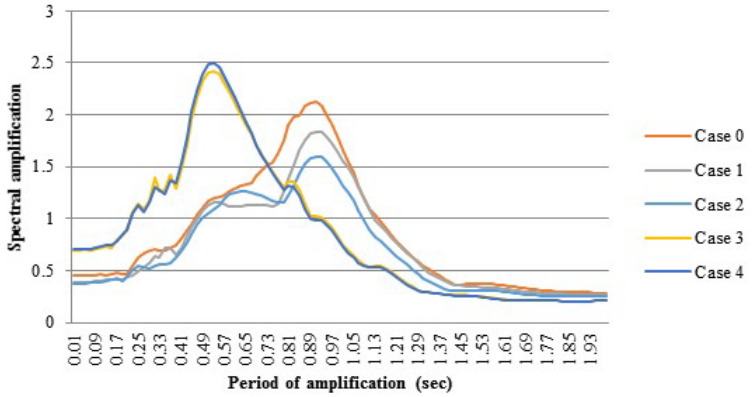

Fig. 5 – Spectral response for each case at point 2

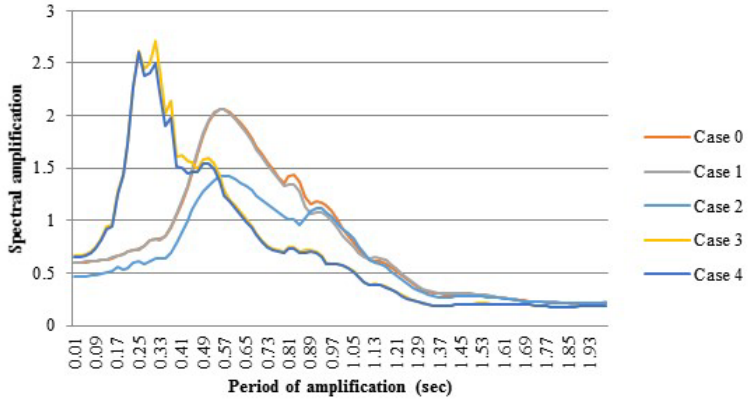

Fig. 6 – Spectral response for each case at point 3

The point 3 is not influenced by the marl layer; indeed its position above the clayey marl layer makes the case 0 and 1 identical. As for the layers in depth, the increase of G_{max} values will produce amplification and a decrease of the value of the period of amplification.

3.1.3 Analyzing the position of the slip circle

The study of the effect of the increase of G_{max} values with the position of the slip circle is very interesting. Fig. 7 shows the different slip circle position and its factor of safety for each case as cited in Table 4.

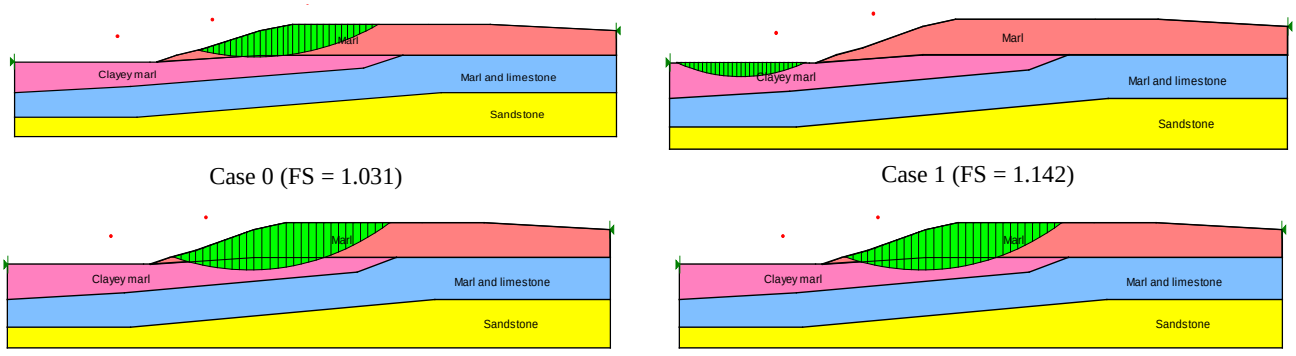

Case 0 (FS = 1.031) Case 1 (FS = 1.142)

Case 2 (FS = 1.145) Case 3 and 4 (FS = 0.629)

Fig. 7 – Slip circle for each case

For case 0, the slip circle is at the interface of the two layers of Marl and Clayey Marl. Increasing the value of G_{max} in the layer 1 (case 1) will move the slip circle to a layer with a lower G_{max}, that is the Clayey Marl layer. In case 2, noting that both surface layers have the same G_{max}, the slip circle will include these two layers, and will not move from its position for the following cases 3 and 4. Therefore, while increasing G_{max} in surface layers and hence decreasing the contrast of surface and deep layers, the factor of safety will increase. On the other hand, while increasing the G_{max} in the deeper layers, the contrast of deep and surface layers will increase and the factor of safety will decrease.

At this stage, we may conclude the following: the more the contrast between dynamic soil proprieties between surface and deep layers is high, the more there is a risk of landslide, and the slip circle will be located at the interface of these two highly contrasted layers.

3.2 Study of G/G_{max} curve and damping ratio

3.2.1 Sensitivity of G/G_{max} curve and damping ratio

The G/G_{max} and damping ratio curves are given by Ishibashi and Zhang [10], as shown in Eq. (5) and Eq. (6).

$$\frac{G}{G_{max}} = 0.5\left(1+\tanh\left(\ln\left(\frac{0.000102+n(IP)}{\gamma}\right)^{0.492}\right)\right)\times \sigma'_m{}^{0.272\left(1-\tanh\left(ln\left(\frac{0.000556}{\gamma}\right)^{0.4}\right)\right)e^{-0.0145\times IP^{1.3}}} \quad (5)$$

$$D = 0.333\frac{1+e^{-0.0145IP^{1.3}}}{2}\left(0.586\left(\frac{G}{G_{max}}\right)^2 - 1.547\frac{G}{G_{max}} + 1\right) \quad (6)$$

Eq. (5) and (6) show a link between the behavior of G/G_{max} and the damping ratio. In order to draw these two curves, confining stress as well as the plasticity index must be calculated. The case 0 as shown in the Table 5 represents the initial values of these two parameters. The remaining cases are the modified values used to study the effects of the G/G_{max} and damping ratio curves. Comparing the evolution of values in Table 5, we notice that from one case to the one following it, values of these parameters are divided approximately by two.

Table 5 – Modification of input values used to calculate G/Gmax and damping ratio curves

Case number	Parameters	Marl	Clayey marl	Marl and limestone	Sand and Silt
0	Confining stress (kPa)	73	107	172	297
	Plasticity index	10	16	14	0
1	Confining stress (kPa)	36	54	86	149
	Plasticity index	5	8	7	0
2	Confining stress (kPa)	18	27	43	75
	Plasticity index	2	4	3	0
3	Confining stress (kPa)	9	13	21	37
	Plasticity index	1	2	1	0

When decreasing the confining stress as well as the plasticity index, the G/G_{max} curves will decrease, as shown in Fig. 8, whereas the damping ratio curve will increase as noticed in Fig. 9, as has been similarly shown [11].

The more G/G_{max} curve decreases, the more the damping ratio increases. The opposite behavior of these two parameters support the relation found by comparing Eq. (5) and Eq. (6).

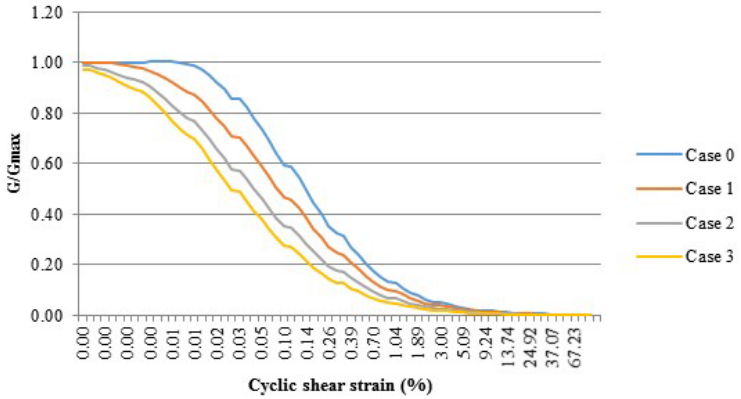

Fig. 8 – G/Gmax curves for the Marl layer for each case

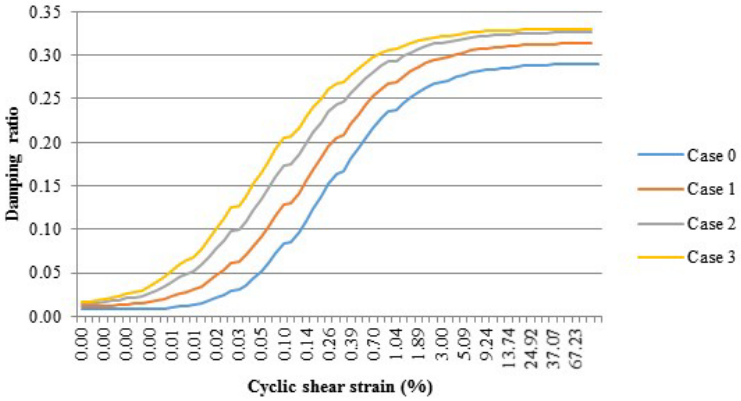

Fig. 9 – Damping ratio curve for the Marl layer

3.2.2 Analyzing amplification in the frequency domain

In order to analyze amplification in the frequency domain, the acceleration spectral response is drawn and the Ratio of Response Spectra (RRS) is calculated for each case and for each point at the surface. Fig.10 to Fig 12 show the RRS for the three points at the surface.

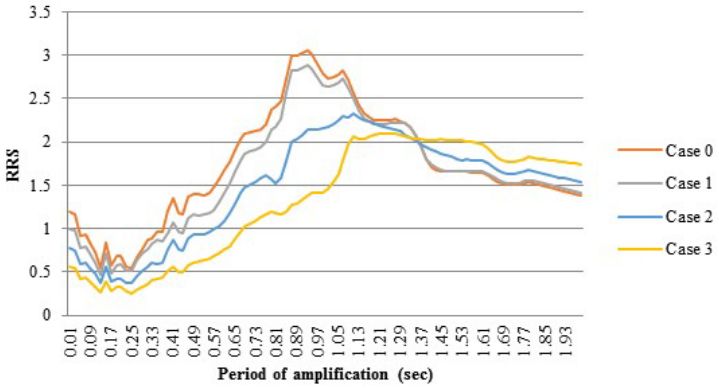

Fig. 10 – RRS at point 1 at the surface for each case

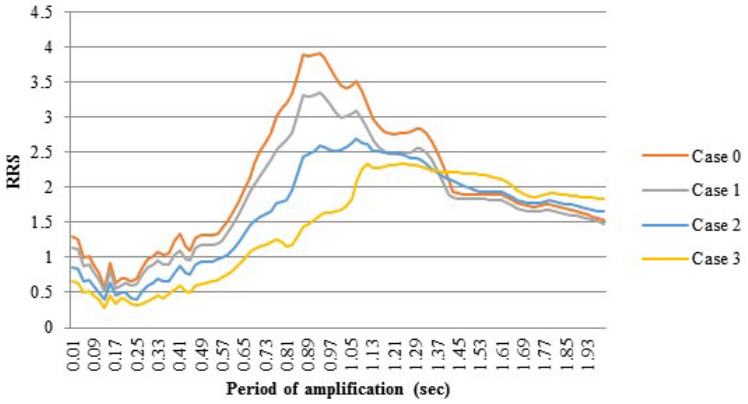

Fig. 11 – RRS at point 2 at the surface for each case

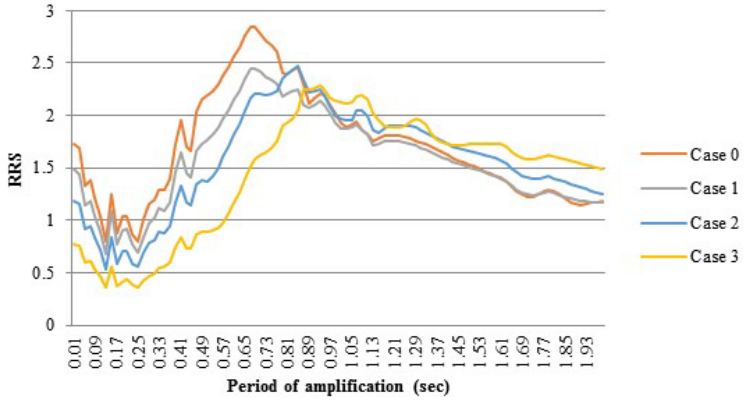

Fig. 12 – RRS at point 3 at the surface for each case

By looking closer at the RRS curves in Fig. 10 to Fig. 12, it seems that the period of amplification has increased whereas the amplification itself shows a decrease, as also shown in Table 6. Indeed, the decrease of the G/G_{max} value will lead to an increase in the period of amplification values, as the increase of the damping ratio will lead to a decrease of the amplification

Table 6 – Amplification and period values for each case

Case	Parameter	Point 1	Point 2	Point 3
0	Period (sec)	0.86	0.86	0.68
	Amplification	3.2	3.7	2.7
1	Period (sec)	0.91	0.91	0.69
	Amplification	2.8	3.3	2.45
2	Period (sec)	1.05	1.05	0.83
	Amplification	2.3	2.7	2.5
3	Period (sec)	1.25	1.21	0.93
	Amplification	2.1	2.3	2.3

3.2.3 Analyzing amplification in the time domain

The difference between maximum surface acceleration compared to maximum acceleration on rock, is related to the nature of soil [12]. Values of a_{max} at the surface after the simulation of an earthquake are gathered in Table 7 below for point 1, 2 and 3.

Table 7 – Amplification, period and a_{max} values for each case

Case	Parameter	Point 1	Point 2	Point 3
0	a_{max} (g)	0.43	0.43	0.59
1	a_{max} (g)	0.35	0.38	0.51
2	a_{max} (g)	0.28	0.3	0.41
3	a_{max} (g)	0.18	0.23	0.23

In initial case 0, the value of a_{max} was amplified at the surface. Indeed, a_{max} for the input was equal to 0.35g, whereas its value according to Table 7 in case 0 is 0.43g for point 1 and 2. Nevertheless, amplification for a_{max} is higher at point 3 compared to points 1 and 2. Therefore, the clayey marl layer leads to a more amplified value of a_{max}. To conclude, in the time domain, clay layers amplify the acceleration much more than granular layers, unlike in the frequency domain, where the opposite trend is observed.

3.2.4 Analyzing the displacement

In order to better understand the impact that dynamic soil properties have on the slope behavior, all resulting relative horizontal displacement during the earthquake are gathered and shown in Fig. 13.

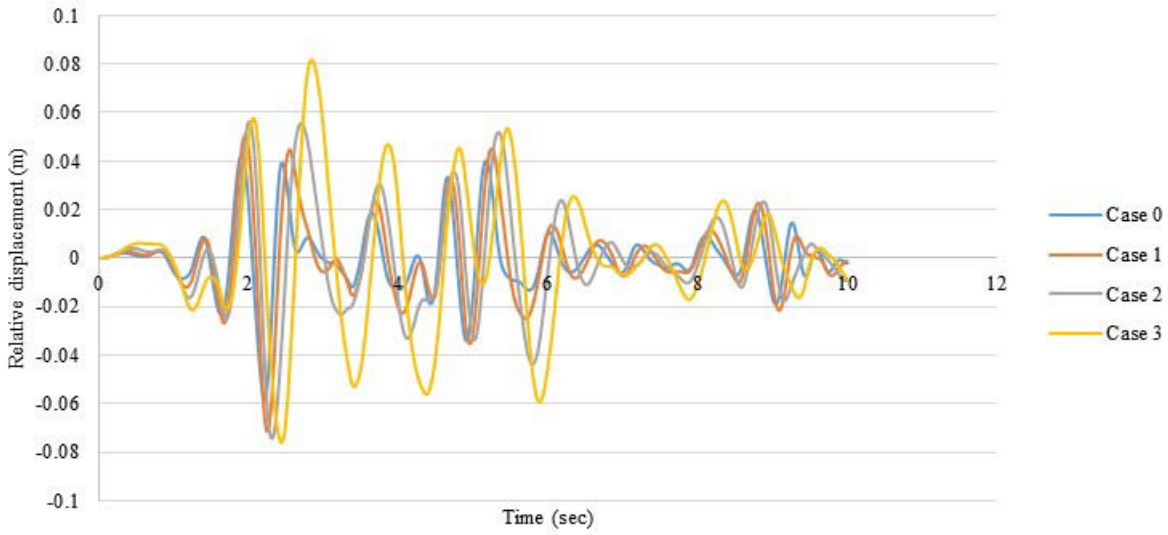

Fig. 13 – Relative displacement for each case

The increase of the damping ratio will lead to a more homogeneous displacement of the slope, which depends less on the shape of the accelerogram. Nevertheless, the displacements seem to be less sudden and take more time to happen, which will lead to a higher factor of safety.

3.2.4 Analyzing the position of the slip circle

For each case mentioned in Table 5, the slip circle has been drawn and the factor of safety calculated as shown in Fig. 14. The position of the slip circle is constant for all cases, whereas the values of the factor of safety decreases while decreasing G/G_{max} and increasing the damping ratio, as shown in Fig. 15.

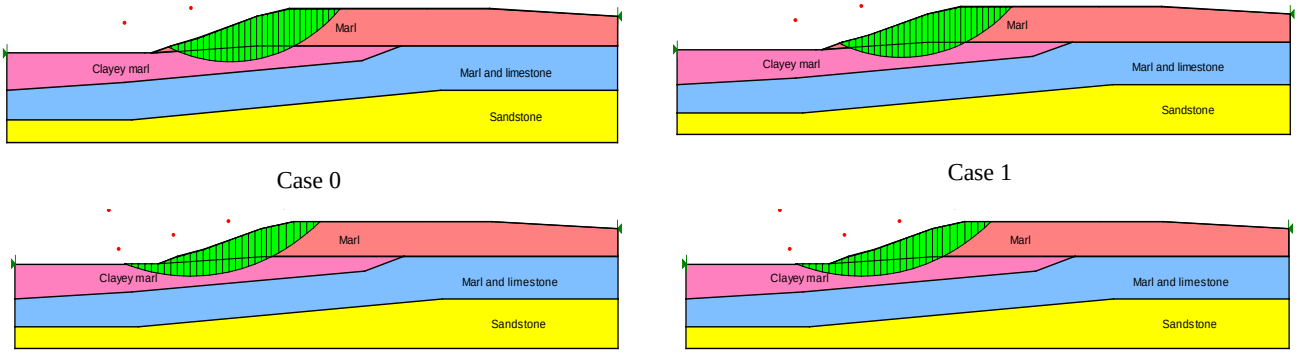

Case 0 Case 1

Case 2 Case 3

Fig. 14 – Position of the slip circle

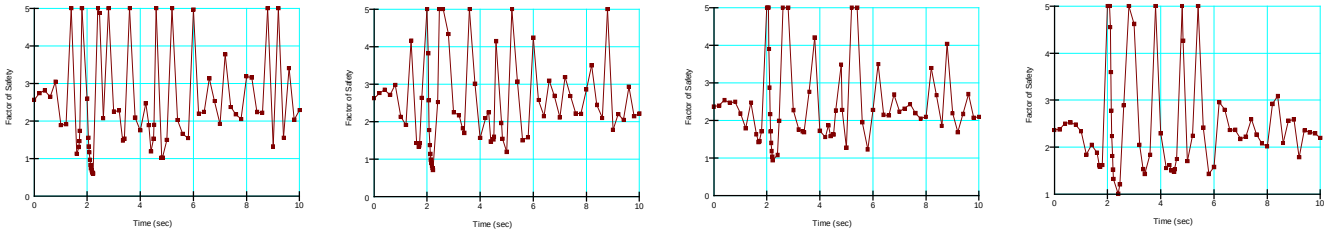

Case 0 (FS = 0.644) Case 1 (FS = 0.711) Case 2 (FS = 0.938) Case 3 (FS = 1.012)

Fig. 15 – Factor of safety vs time

The more the damping ratio increases and the G/G_{max} curve decreases, the more the values of the factor of safety will increase. As we have seen earlier, the amplification is decreasing, and will lead to a higher factor of safety. Nevertheless, the position of the slip circle is still the same for all the cases, unlike in earlier cases. Indeed, by leaving the highly contrasted interface between the surface and deeper layer of soil, the slip circle will not choose a better-contrasted interface.

4. Conclusion

Knowledge of the soil nature is essential to determine the behavior of a soil during an earthquake. In the aim of understanding the role of dynamics soil parameters, a parametric study has been carried out. As we increase the G_{max} values of the surface layers, we noticed that the slip circle was occurring in a less stiff layer of soil and a highly contrasted interface. The increase of G_{max} values in deeper soil will not lead to the displacement of the slip surface, but will decrease the values of the factor of safety up to 55% of its initial value.

On the other hand, the decrease of G/G_{max} and increase of the damping ratio will decrease the amplification values, and lead to an rise in the factor of safety. Also, the amplification has been analyzed with respect to whether the soil was rather cohesive or granular.

The results obtained in this paper will certainly help the scientific community understand the behavior of soils in seismic situation, and will help the RUMMARE project to better interpret the causes of landslides on the Pan Arab highway at Dahr el Baidar area and give them an idea of what could happen to slopes during an earthquake. More specific results are forthcoming.

5. Acknowledgements

We would like to acknowledge the contribution to the present work of the research unit RUMMARE, a Research Unit on Mass Movement hazard Assessment and Risk Evaluation grouping researchers from major universities and research centers in Lebanon, with the following researchers being the principal investigators: J. Harb, M.E. Rahhal, D. Youssef Abdel Massih, F. Hage Chehade, C. Abdallah, E. Ibrahim, L. Khalaf Keyrouz, G. Nasr, and A. Sursock. The researchers would like to thank the Lebanese National Council for Scientific Research for funding this unit.

6. References

[1] Popescu ME (2002): Landslide causal factors and landslide remedial options. Keynote Lecture. *Proceedings of the third international conference on landslides, slope stability and safety of infrastructures,* Singapore: 61-81.

[2] Rahhal ME, Nini R, Favre JL (2003): Analysis of Factors Causing Slope Instabilities. *Proceedings 56th Canadian Geotechnical Conference*, Winnipeg, CANADA, Volume 2, 368-375.

[3] Rahhal ME, Nini R, Favre JL (2004): Une Approche Simple de la Cartographie du Risque du Glissement de Terrains. *Proceedings of the 57th Canadian Geotechnical Conference*, Québec, Canada, Session 5C, pp. 13-18.

[4] Rahhal ME, Masaad N (2008): Comprendre le comportement d'une couche savon dans un glissement de terrain, *Proceedings 61st Canadian Geotechnical Conference*, Edmonton, Alberta, CANADA, pages 477-484.

[5] Huijer C, *Harajli* M, Sadek S (2011): Upgrading the seismic hazard of Lebanon in light of the recent discovery of the offshore thrust fault system, *Lebanese Science Journal*, **12** (2), Beirut, Lebanon.

[6] Day R (2001): *Geotechnical Earthquake Engineering Handbook*, McGraw-Hill Handbooks.

[7] Seed HB, Idriss IM (1970): Soil moduli and damping factors for dynamic response analysis, *Report No. EERC 70-10*, University of California, Berkeley.

[8] Mayne P, Rix G (1995): Laboratory and field determinations of small-strain shear modulus for a structured Champlain clay, *Canadian Geotechnical Journal*, **32** (1), 193 – 194, Canada.

[9] Mohraz B (1976): A study of earthquake response spectra for different geological conditions, *Bulletin of the Seismological Society of America*, **66** (3), 915 – 935.

[10] Ishibashi I, Zhang X (1993): Unified dynamic shear moduli and damping ratios of sand and clay, *Japanese Society of Soil Mechanics and Foundation Engineering*, **33** (1), 182 –191, Japan.

[11] Kokusho T (1980): Cyclic triaxial test of dynamic soil properties for wide strain range, *Soils and Foundations*, **20** (3), 46 – 60.

[12] Kumar K (2008): Basic Geotechnical earthquake engineering, *New age international publishers*, New Delhi, India.